Supporting Information for

A Ligand-Incorporating Strategy towards Single-Component White Light in Ionic Zero-Dimensional Indium Chlorides

Hao-Wei Lin,[a,b] Abdusalam Ablez,[a,b] Zhong-Hua Deng,[a] Zhi-Hua Chen,[a,c] Ying-Chen Peng,[a,c] Ze-Ping Wang,[a*] Ke-Zhao Du[d*] and Xiao-Ying Huang[a,c*]

Affiliations:

[a]State Key Laboratory of Structural Chemistry, Fujian Institute of Research on the Structure of Matter, Chinese Academy of Sciences, Fuzhou, Fujian 350002, P. R. China.

[b]College of Chemistry, Fuzhou University, Fuzhou 350108, P. R. China

[c]University of Chinese Academy of Sciences, Beijing 100049, P. R. China.

[d]Fujian Provincial Key Laboratory of Advanced Materials Oriented Chemical Engineering, Fujian Normal University, 32 Shangsan Road, Fuzhou 350007, P. R. China.

Experimental section

Materials

All purchased reagents were utilized directly without further purification. The detailed information for the reagents is listed as follows: 1-Ally-2,3-dimethylimidazolium chloride ([Ammim]Cl, 98%, Lanzhou Greenchem ILs, Lanzhou, China); 4,4'-dimethyl-2,2'-bipyridyl (dmbp, 98%, Adamas); indium (III) chloride tetrahydrate ($InCl_3 \cdot 4H_2O$, 99.99%, 9dingchem); acetonitrile (CH_3CN, AR, Sinopharm Chemical Reagent Co., Ltd., Shanghai, China).

Synthesis

Synthetic methods: [Ammim][$InCl_4$(dmbp)] were synthesized by the solvothermal process. Firstly, the mixture of $InCl_3 \cdot 4H_2O$ (1 mmol, 0.294 g), dmbp (1 mmol, 0.185 g), [Ammim]Cl (1 mmol, 0.173 g), and CH_3CN (5 mL) was added into a 28 mL Teflon-lined steel autoclave. Then, the Teflon-lined steel autoclave was put into the oven for heating. Then, the reactor was heated at 140 °C for 4 days and cooled slowly to ambient temperature in 2 days. After allowing it to naturally cool to room temperature (RT), yellowish block crystals were obtained. The yield was calculated to be nearly 85.8% based on In atom. EA: Calcd (%): C, 41.55; H, 4.35; N, 9.69. Found (%): C, 41.57; H, 4.50; N, 9.67.

Characterization methods

Single Crystal X-ray diffraction (SCXRD): A suitable crystal was selected under an optical microscope for the measurement of SCXRD. Intensity data were measured and collected on a Rigaku HyPix-6000HE diffractometer equipped with graphite-monochromated GaK_α radiation (λ = 1.34140 Å) at 298 K. The structure was solved by direct methods and refined by full-matrix least-squares on F^2 using the SHELX-2018 program package.[1] All non-H atoms were refined anisotropically, and the H atoms attached to C atoms were located at geometrically calculated positions. The empirical formula was verified by elemental analysis.

Powder X-ray diffraction (PXRD)*:* The experimental PXRD patterns were measured by Rigaku Miniflex-II diffractometer by utilizing CuK_α radiation (λ = 1.54178 Å) in the angular range of 2θ =

5 - 50°. The simulated PXRD pattern was calculated by using the single crystal X-ray structural data at RT *via* Mercury software.

Thermogravimetric analyses (TGA): TG curve was recorded on a NETZSCH STA 449F3 instrument with a heating rate of 10 $K \cdot min^{-1}$ under the N_2 atmosphere.

UV-visible absorption spectroscopy (UV-vis): Steady-state UV-vis was recorded on a Shimadzu 2600 UV/vis spectrometer at room temperature (RT) in the range of 800-200 nm. The $BaSO_4$ plate was utilized as a standard which possesses 100% reflectance. The absorption data was then obtained from the reflectance spectra by using the Kubelka-Munk function $\alpha/S = (1 - R)^2/2R$, where α refers to the absorption coefficient, S refers to the scattering coefficient, and R refers to the reflectance.[2]

Photoluminescence Characterization: Photoluminescence excitation (PLE), photoluminescence emission (PL) spectra, PL decay spectra and photoluminescent quantum yields (PLQY) were measured on FLS1000 UV/V/NIR fluorescence spectrometer. Temperature-dependent PL spectra were measured on an FLS980 UV/V/NIR fluorescence spectrometer with temperatures ranging from 77 K to 300 K.

WLED Performance: The device WLED was fabricated by coating the mixture of [Ammim][$InCl_4$(dmbp)] and silicone on the commercial 380 nm InGaN chip (San'an Optoelectronics CO., LTD.). The photoelectric properties of the WLEDs were measured by HAAS-2000 integrating sphere spectroradiometer system (Everfine, China).

Density Functional Theory (DFT) Calculations: According to the single-crystal structure refinement results, DFT calculations of [Ammim][$InCl_4$(dmbp)] were implemented in the Vienna ab initio simulation package (VASP).[3, 4] The generalized gradient approximation (GGA) for the exchange-correlation term with the Perdew-Burke-Ernzerhof (PBE) exchange-correlation functional was applied for electron-electron exchange correlation processes.[5] Projected augmented wave (PAW) potentials were used with the valence states 2s and 2p for C and N, 5s and 5p for In, 3s and 3p for Cl. To ensure sufficient accuracy, the cut-off energy of 500 eV for the plane wave expansion was chosen, self-consistent field (SCF) computations were set to a convergence criterion of 1×10^{-5} eV and the force criterion was 0.02 eV $Å^{-1}$.

Crystallographic data

Table S1. Crystal data and structure refinement for [Ammim][$InCl_4$(dmbp)] .

CCDC number	2311862
Empirical formula	$C_{20}H_{25}Cl_4InN_4$
Formula weight	578.06
Temperature/K	298(2)
Wavelength/Å	1.34140
Crystal system	Monoclinic
Space group	$P2_1/c$
a/Å	12.3933(2)
b/Å	13.3229(2)
c/Å	15.3602(2)
α/°	90
β/°	109.006(2)
γ/°	90
Volume/Å^3	2397.93(7)
Z	4
ρ_{calc} g/cm^3	1.601
Absorption coefficient/mm^{-1}	8.174
F(000)	1160
Crystal size/mm^3	0.200×0.100×0.020
Theta range for data collection /°	3.279 - 60.046
Reflections collected/ unique	17775/5305 [R_{int} = 0.0346]
Refinement method	Full-matrix least-squares on F^2
Data/restraints/parameters	5305/0/267
Goodness-of-fit on F^2	1.062
Final R indexes [$I >= 2\sigma(I)$]	R_1[a] = 0.0279, wR_2[b] = 0.0722
Final R indexes [all data]	R_1[a] = 0.0311, wR_2[b] = 0.0740
Largest diff. peak and hole	0.743/-0.929

[a] $R_1 = \sum \| F_o | - | F_c \| / \sum | F_o |$, [b] $wR_2 = [\sum w(F_o^2 - F_c^2)^2 / \sum w(F_o^2)^2]^{1/2}$

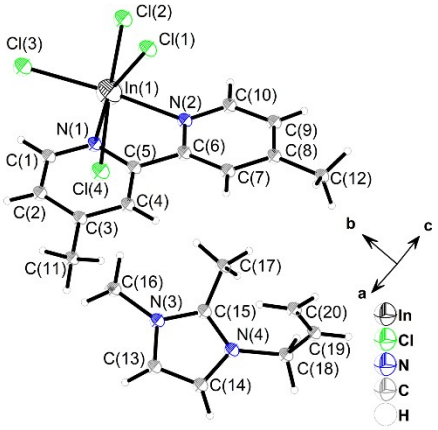

Figure S1. *ORTEP* drawing (50% ellipsoid probability) of the asymmetric units of [Ammim][$InCl_4$(dmbp)].

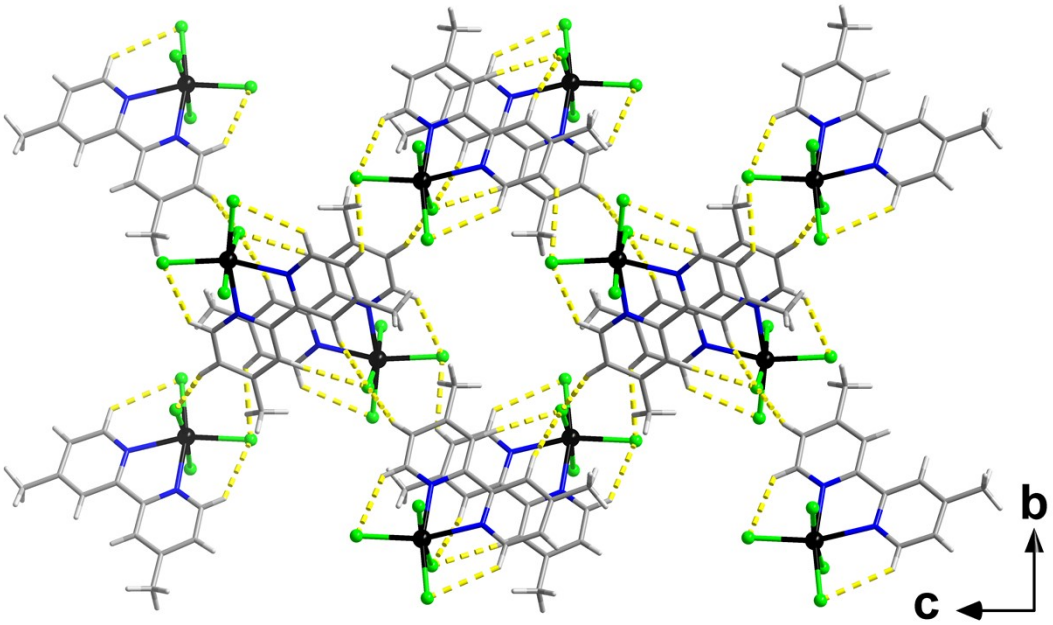

Figure S2. The diagram of anionic units connected by hydrogen bonds (yellow dotted line) viewed along the *a* axis.

Table S2. Selected bond lengths (Å) and bond angles (°) for [Ammim][$InCl_4$(dmbp)].

In(1)-N(2)	2.3026(19)	In(1)-Cl(1)	2.4573(6)
In(1)-N(1)	2.3078(17)	In(1)-Cl(4)	2.5079(7)
In(1)-Cl(3)	2.4349(6)	In(1)-Cl(2)	2.5095(6)
N(2)-In(1)-N(1)	71.24(6)	Cl(1)-In(1)-Cl(4)	91.19(2)
N(2)-In(1)-Cl(3)	166.23(5)	N(1)-In(1)-Cl(1)	163.91(5)
N(1)-In(1)-Cl(3)	95.85(5)	N(2)-In(1)-Cl(4)	89.27(5)
N(2)-In(1)-Cl(1)	93.79(5)	N(1)-In(1)-Cl(4)	82.96(5)

Symmetry transformations used to generate equivalent atoms: N.A.

Table S3. Hydrogen bonds for [Ammim][$InCl_4$(dmbp)].

D-H···A	*d*(D-H)	*d*(H···A)	*d*(D···A)	<(DHA)
C(1)-H(1A)···Cl(3)	0.93	2.90	3.542(3)	127.1
C(2)-H(2A)···Cl(1)#1	0.93	2.84	3.514(3)	130.2
C(4)-H(4A)···Cl(2)#2	0.93	2.93	3.785(3)	152.8
C(7)-H(7A)···Cl(2)#2	0.93	2.71	3.592(2)	159.6
C(9)-H(9A)···Cl(2)#3	0.93	2.82	3.662(3)	150.5
C(10)-H(10A)···Cl(1)	0.93	2.86	3.496(3)	126.9
C(13)-H(13A)···Cl(3)#4	0.93	2.84	3.541(3)	132.7
C(14)-H(14A)···Cl(1)#5	0.93	2.85	3.632(3)	142.5
C(17)-H(17B)···Cl(4)#6	0.96	2.77	3.691(3)	160.7
C(18)-H(18A)···Cl(4)#6	0.97	2.95	3.839(3)	152.1
C(18)-H(18B)···Cl(1)#5	0.97	2.93	3.655(3)	132.3

Symmetry transformations used to generate equivalent atoms: #1 *x*, -*y*+3/2, *z*-1/2 #2 -*x*, -*y*+1, -*z*+1 #3 -*x*-1, *y*-1/2, -*z*+3/2 #4 -*x*+1, -*y*+1, -*z*+1 #5 *x*, -*y*+1/2, *z*-1/2 #6 -*x*+1, *y*-1/2, -*z*+3/2

Table S4. Selected π···π interactions data for [Ammim][$InCl_4$(dmbp)].

Cg((I)···Cg((J)	ARU(J)	Cg···Cg(Å)	α(°)	β(°)	γ(°)
Cg(2)→Cg(3)	[3566.01]	3.7883(15)	6.52(12)	19.1	25.0
Cg(3)→Cg(2)	[3566.01]	3.7885(15)	6.52(12)	25.0	19.1

[3566] = -*x*, 1-*y*, 1-*z*; Cg(2): N(1) →C(1) →C(2) →C(3) →C(4) →C(5); Cg(3): N(2) →C(6) →C(7) →C(8) →C(9) →C(10)

Table S5. Selected C-H···π interactions data for [Ammim][$InCl_4$(dmbp)].

C-H(I)→Cg(J)	ARU(J)	H···Cg(Å)	＜X···Cg (°)	X···Cg(Å)	X-H, Pi
C(20)-H(20A)→Cg(4)	[1555.02]	2.95	123	3.545(4)	1

[1555] = *x*, *y*, *z*; Cg(4): N(3) →C(13) →C(14) →N(4) →C(15)

Table S6. Selected anion···π interactions data for [Ammim][$InCl_4$(dmbp)].

Y-X(I)→Cg(J)	ARU(J)	X···Cg(Å)	Y-X···Cg (°)	Y···Cg(Å)	Y-X, Pi
In(1)-Cl(1)→Cg(4)	[2656.02]	3.4933(15)	122.63(4)	5.2440(13)	24.84

[2656] = 1-*x*, 1/2+*y*, 3/2-*z*; Cg(4): N(3) →C(13) →C(14) →N(4) →C(15)

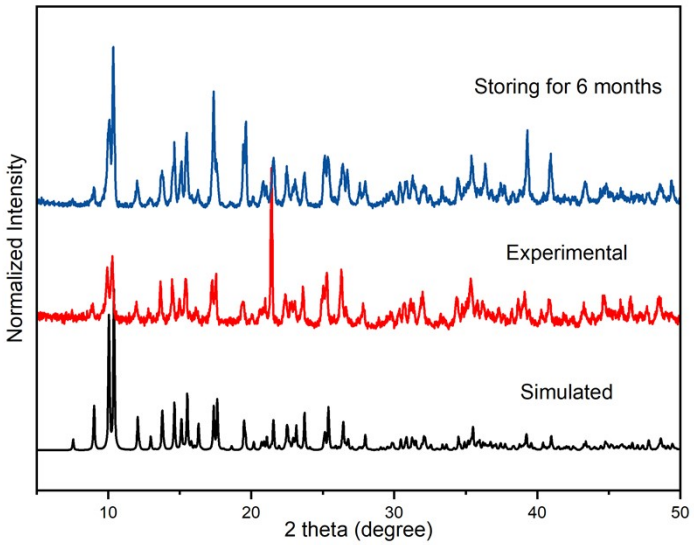

Figure S3. The experimental PXRD patterns for as-made [Ammim][$InCl_4$(dmbp)] and that storing at ambient conditions for six months compared with the one simulated from SCXRD data.

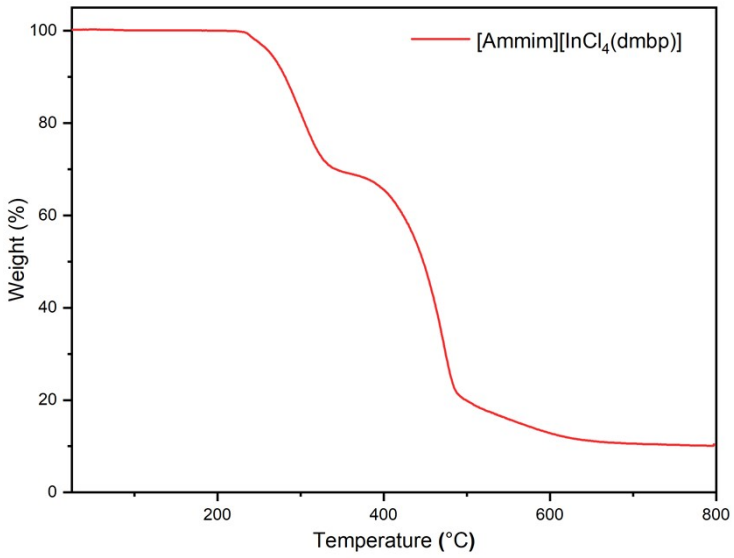

Figure S4. The TG curve for [Ammim][$InCl_4$(dmbp)].

Table S7. Properties of some single-component white light-emitting materials in recent years.

Compound	PLQY (%)	CIE (*x*,*y*)	CRI	CCT (K)	Ref.
[Ammim][$InCl_4$(dmbp)]	16.70	0.3269, 0.3461	93.2	5744	This work
$InCl_3$-TPOBD	10.50	0.28, 0.33	84.8	9370	6
$(H_2AMP)CdBr_4 \cdot H_2O$	23.46	0.36, 0.38	98.0	--	7
(EDBE)$PbBr_4$	2.16	0.39, 0.42	84.0	3990	8
(PEPC)$PbCl_4$	2.10	0.37, 0.42	84.0	4426	9
BIF-142-Cl	16.00	0.312, 0.335	90.4	5364	10
$DPCu_4I_6$	89.76	0.36, 0.35	85.1	4415	11
$(C_{12}H_{24}O_6)CsCu_2Br_3$	78.30	0.3397, 0.4280	73.7	4962	12
$(TMPA)_2SnCl_6$	3.88	0.31, 0.35	86.7	5390	13
(3APr)$PbCl_4$	--	0.47, 0.45	85	2835	14
(3APr)$PbBr_4$	--	0.43, 0.45	83	3456	14
(3APr)PbI_4	--	0.40, 0.47	77	4122	14
γ-MPAPB	6.85	0.22, 0.23	85	53281	15
PhPz-In	18.56	0.34, 0.34	89	5244	16
AMPd-In	18.21	0.31, 0.33	85	4770	16
AEPz-In	7.01	0.29, 0.35	84	8149	16
$(C_{12}H_{18}N_6)Pb_2Cl_{10} \cdot H_2O$	1.00	0.31, 0.33	93.4	6512	17
$[C_4N_2H_{12}]_3[PbBr_5]_2 \cdot 4DMSO$	59.00	0.3554, 0.4227	78	4897	18
ATZ2	4.80	0.28, 0.34	73	8401	19
TPMI-Br	28.3	0.32, 0.36	85.5	6004	20
TIM	11.8	0.33, 0.35	85	5669	21
1	2	0.31, 0.35	83	6218	22

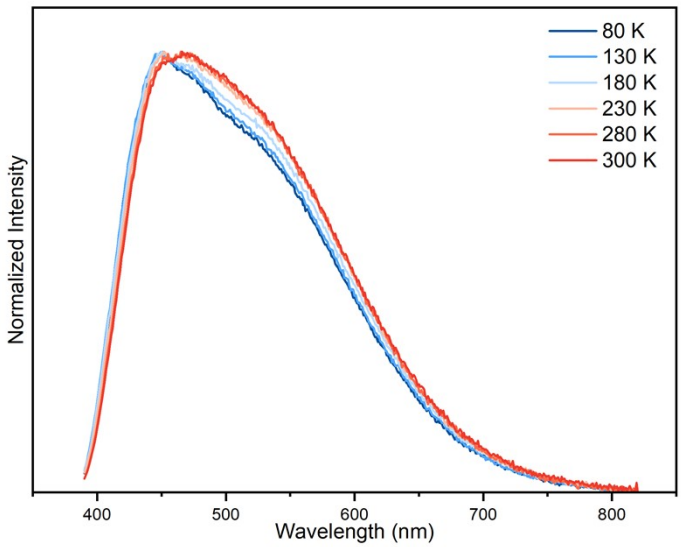

Figure S5. Temperature-dependent PL spectra of [Ammim][$InCl_4$(dmbp)] under 375 nm excitation.

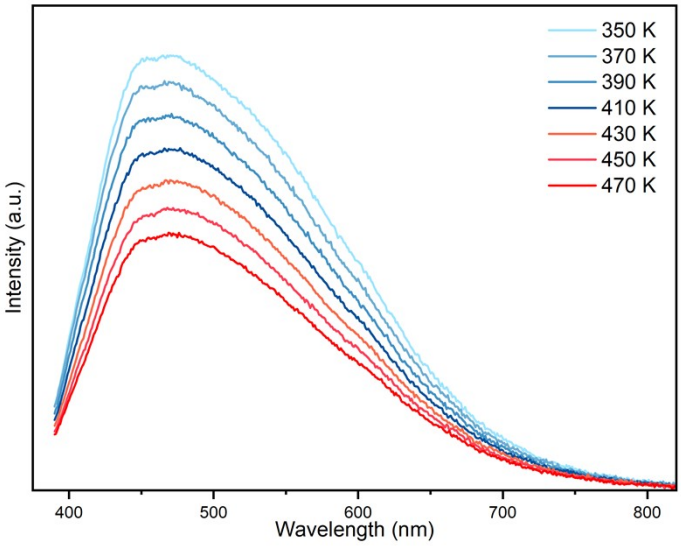

Figure S6. Temperature-dependent PL spectra of [Ammim][$InCl_4$(dmbp)] under 375 nm excitation at 350 K to 470 K.

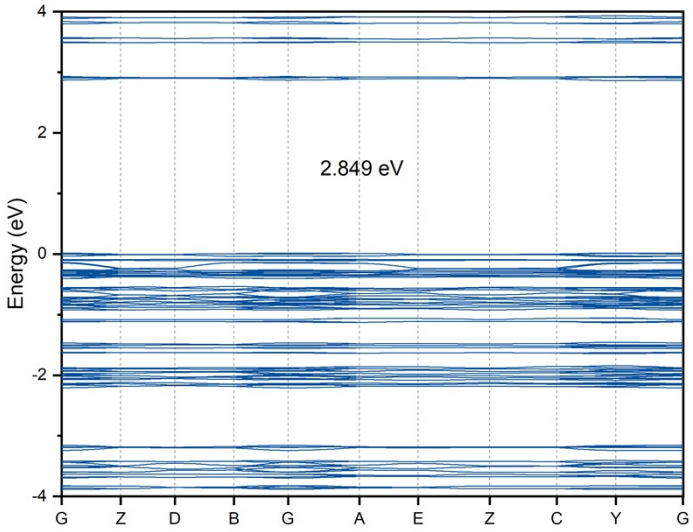

Figure S7. The electronic band structure of [Ammim][$InCl_4$(dmbp)]. The calculated bandgap of [Ammim][$InCl_4$(dmbp)] is 2.849 eV.

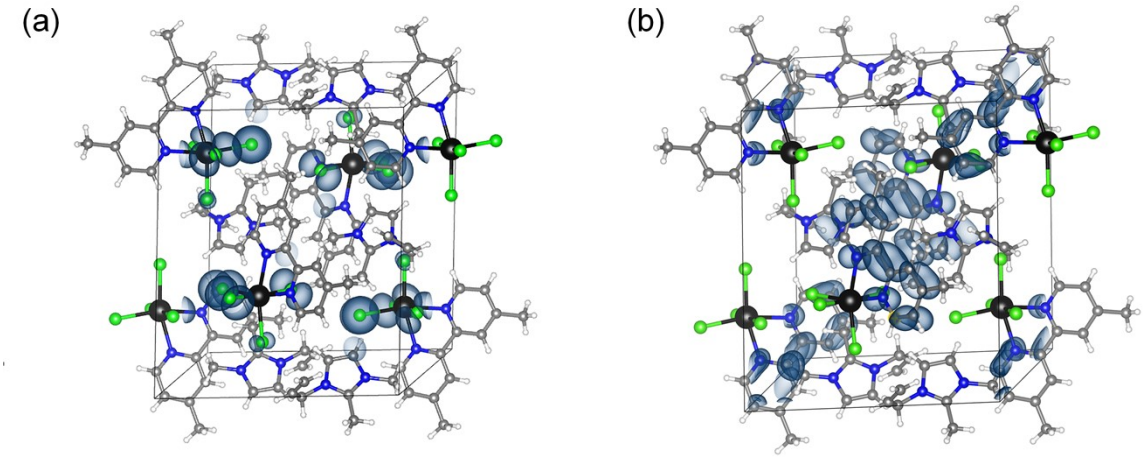

Figure S8. The calculated orbital-resolved DOSs of [Ammim][$InCl_4$(dmbp)]. The highest occupied molecular orbital (HOMO, a) and lowest occupied molecular orbital (LUMO, b).

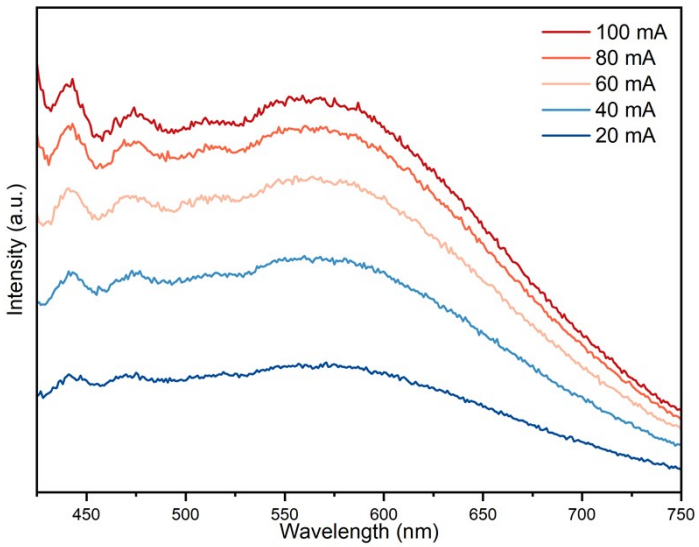

Figure S9. The emission spectra of WLED fabricated with [Ammim][$InCl_4$(dmbp)] coating on InGaN UV chip (λ_{em} = 380 nm) from 20 to 100 mA.

Table S8. Photoelectric parameters of the fabricated WLED under various currents.

Current (mA)	CCT	CRI	CIE	LE (lm/W)
20	5336	93.7	0.3369, 0.3601	0.98
40	5444	93.7	0.3340, 0.3570	0.85
60	5558	93.8	0.3311, 0.3534	0.73
80	5646	93.8	0.3290, 0.3500	0.62
100	5744	93.2	0.3269, 0.3461	0.52

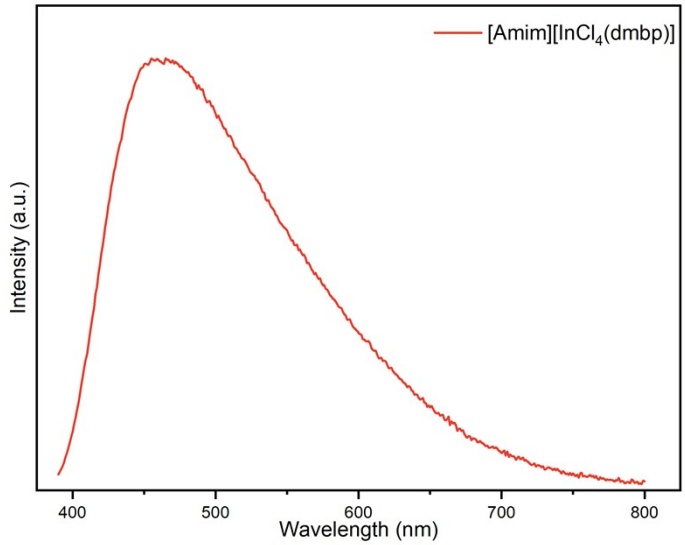

Figure S10. The emission spectrum of [Amim][$InCl_4$(dmbp)] at 375 nm excitation.

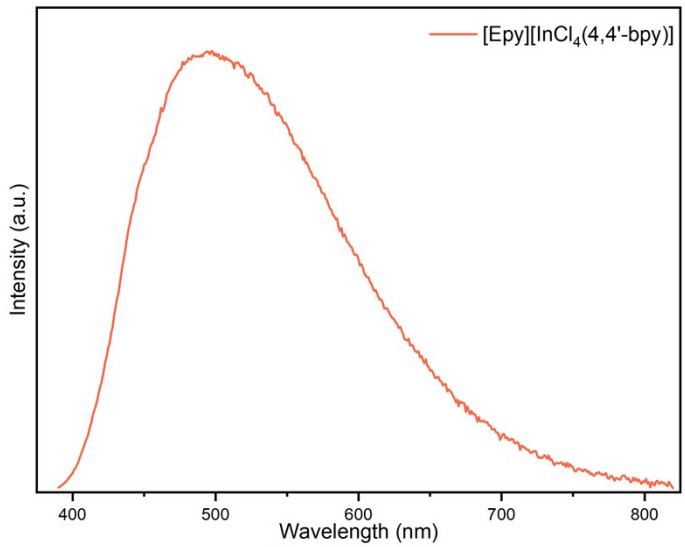

Figure S11. The emission spectrum of [Epy][$InCl_4$(4,4'-bpy)] at 375 nm excitation.

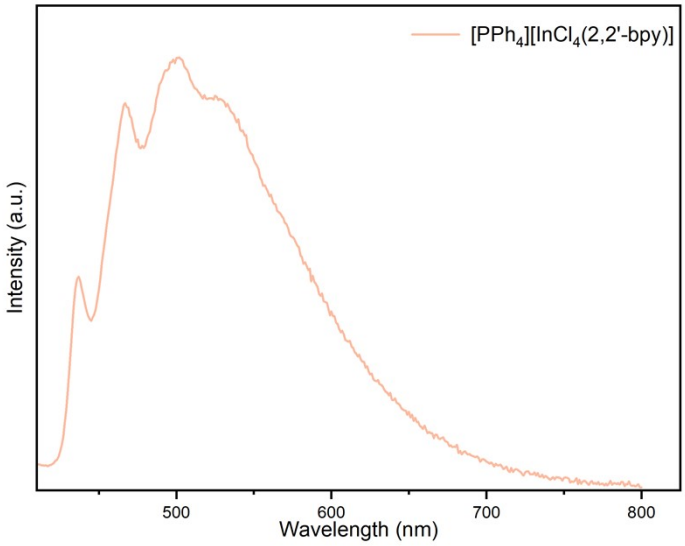

Figure S12. The emission spectrum of [PPh_4][$InCl_4$(2,2'-bpy)] at 328 nm excitation.

References:

1. G. M. Sheldrick, *Acta Crystallogr. Sect. C-Struct. Chem.*, 2015, **71**, 3-8.
2. W. M. Wendlandt and H. G. Hecht, *New York*, 1966.
3. G. Kresse and J. Hafner, *Phys. Rev. B*, 1993, **48**, 13115-13118.
4. G. Kresse and J. Furthmuller, *Phys. Rev. B*, 1996, **54**, 11169-11186.
5. J. P. Perdew, K. Burke and M. Ernzerhof, *Phys. Rev. Lett.*, 1996, **77**, 3865-3868.
6. T. Chen, Y.-J. Ma and D. Yan, *Adv. Funct. Mater.*, 2023, **33**, 2214962.
7. H. Gao, Z. Lu, X. Zhao, K. Zhang, X. Zhu, R. Cheng, S.-L. Li, Z. Qi and X.-M. Zhang, *J. Mater. Chem. C*, 2023, **11**, 9023-9029.

8. E. R. Dohner, A. Jaffe, L. R. Bradshaw and H. I. Karunadasa, *J. Am. Chem. Soc.*, 2014, **136**, 13154-13157.
9. K. Thirumal, W. K. Chong, W. Xie, R. Ganguly, S. K. Muduli, M. Sherburne, M. Asta, S. Mhaisalkar, T. C. Sum, H. S. Soo and N. Mathews, *Chem. Mater.*, 2017, **29**, 3947-3953.
10. Z.-R. Wang, J.-Q. Chen, Q.-H. Li, H.-X. Zhang and J. Zhang, *Adv. Opt. Mater.*, 2023, **11**, 2202743.
11. S. Zhou, Y. Chen, K. Li, X. Liu, T. Zhang, W. Shen, M. Li, L. Zhou and R. He, *Chem. Sci.*, 2023, **14**, 5415-5424.
12. J. Huang, Y. Peng, J. Jin, M. S. Molokeev, X. Yang and Z. Xia, *J. Phys. Chem. Lett.*, 2021, **12**, 12345-12351.
13. Q.-F. Luo, H.-F. Ni, P.-Z. Huang, M. Zhu, C.-F. Wang, Q.-H. Zhuo, D.-W. Fu, Y. Zhang and Z.-X. Zhang, *Mater. Chem. Front.*, 2023, **7**, 6247-6253.
14. X. Li, P. Guo, M. Kepenekian, I. Hadar, C. Katan, J. Even, C. C. Stoumpos, R. D. Schaller and M. G. Kanatzidis, *Chem. Mater.*, 2019, **31**, 3582-3590.
15. Y. Li, C. Ji, L. Li, S. Wang, S. Han, Y. Peng, S. Zhang and J. Luo, *Inorg. Chem. Front.*, 2021, **8**, 2119-2124.
16. D.-Y. Li, Y.-M. Sun, X.-Y. Wang, N.-N. Wang, X.-Y. Zhang, C.-Y. Yue and X.-W. Lei, *J. Phys. Chem. Lett.*, 2022, **13**, 6535-6643.
17. D. Li, W. Wu, S. Wang, X. Zhang, L. Li, Y. Yao, Y. Peng and J. Luo, *J. Mater. Chem. C*, 2020, **8**, 6710-6714.
18. G. Yu, F. Lin, K. Zhou, S. Fang, Y. Shi, W. Liu, H. Hu, B. Ma and H. Lin, *Chem. Mater.*, 2021, **33**, 5668-5674.
19. Y. Song, L. Hu, Q. Cheng, Z. Chen, H. Su, H. Liu, R. Liu, S. Zhu and H. Zhu, *J. Mater. Chem. C*, 2022, **10**, 6392-6401.
20. J. Zhang, P. Alam, S. Zhang, H. Shen, L. Hu, H. H. Y. Sung, I. D. Williams, J. Sun, J. W. Y. Lam, H. Zhang and B. Z. Tang, *Nat. Commun.*, 2022, **13**, 3492.
21. X. Zheng, Y. Huang, D. Xiao, S. Yang, Z. Lin and Q. Ling, *Mater. Chem. Front.*, 2021, **5**, 6960-6968.
22. N.-N. Zhang, C. Sun, X.-M. Jiang, X.-S. Xing, Y. Yan, L.-Z. Cai, M.-S. Wang and G.-C. Guo, *Chem. Commun.*, 2017, **53**, 9269-9272.